X-ray Diffraction Study of Liquid Cs up to 9.8 GPa

S. Falconi, L. F. Lundegaard, C. Hejny, and M. I. McMahon

School of Physics and Centre for Science at Extreme Conditions, The University of Edinburgh, Mayfield Road, Edinburgh, EH9 3JZ, United Kingdom

(Received 30 November 2004; published 1 April 2005)

We describe an x-ray diffraction study of liquid Cs at high pressure and temperature conducted in order to characterize the structural changes associated with the complex melting curve and phase transitions observed in the solid phases. At 3.9 GPa we observe a discontinuity in the density of the liquid accompanied by a decrease in the coordination number from about 12 to 8, which marks a change to a nonsimple liquid. The specific volume of liquid Cs, combined with structural analysis of the diffraction data, strongly suggest the existence of dsp^3 electronic hybridization above 3.9 GPa, similar to that reported on compression in the crystalline phase.

DOI: 10.1103/PhysRevLett.94.125507 PACS numbers: 61.10.Nz, 61.20.–p, 61.25.Mv

Cs has one of the most interesting pressure-temperature (P-T) phase diagrams of all the elements. It exhibits numerous solid phases with very different bulk modulii, and a melting curve whose gradient varies dramatically with pressure (see Fig. 1) [1,2]. At ambient conditions Cs-I has the eightfold coordinated bcc structure and this transforms to 12-coordinated fcc Cs-II at 2.4 GPa. At 4.2 GPa, the close-packed Cs-II transforms to Cs-III, which was long thought to also have an fcc structure, but which has a complex orthorhombic structure with 84 atoms in a C-centered unit cell [3]. Cs-III is ninefold or tenfold coordinated and exists over only a very narrow pressure range, and at 4.4 GPa transforms to eightfold coordinated tetragonal Cs-IV. The Cs-II $\rightarrow$ Cs-III $\rightarrow$ Cs-IV transition sequence is accompanied by abrupt changes in resistivity [1] and this phenomenon has been attributed to the collapse of the 6s electronic orbital onto the 5d orbitals (so called s-to-d electron transfer) [4]. The Cs melting curve exhibits abrupt changes in slope with pressure; initially it shows a positive slope and there are two maxima at 2.25 GPa and $T_m = 197\,^{\circ}\mathrm{C}$ and 3.05 GPa and $T_m = 198\,^{\circ}\mathrm{C}$ [1]. On further pressure increase, the gradient of the melting curve becomes strongly negative until the Cs-II–Cs-III–liquid triple point, where it becomes almost constant at $T_m = 88\,^{\circ}\mathrm{C}$ before again becoming strongly positive at pressures above the Cs-III–Cs-IV–liquid triple point up to 9.8 GPa, the highest pressure at which it has been determined [1,5]. As with the solid phases, the changes in the melting curve are accompanied by changes in resistivity of the liquid [1]. But these changes are more continuous than those observed in the solid and this led early studies of l-Cs to conclude that if s-to-d transfer occurs in the liquid, then the mechanism is different from that found in the solid [1]. Further studies by Tsuji *et al.* [6] have suggested that the structural changes in the liquid are similar to those in the solid [1], with a change from a bcc-like structure to an fcc-like structure at 2.0 GPa, and a decrease in the coordination number between 2.9 and 4.3 GPa. However, the data in this study were collected at only four P-T points, and the maximum pressure achieved, 4.3 GPa, was not high enough to investigate the liquid above the Cs-IV phase.

In order to investigate the structure of l-Cs across the strong discontinuity in the melting curve at 4.4 GPa, and to further explore the structural changes in the liquid that accompany the known complex changes in the crystalline structure, we have conducted detailed x-ray diffraction studies up to 9.8 GPa at 220 °C and 350 °C, a factor of more than two higher in pressure than the earlier studies [6]. We observe significant densification of the liquid over this pressure range accompanied by a discontinuity in the density, and a change in coordination from 11–12 to 7–8, behavior that closely follows that observed in the solid phases. The P-T points at which we have collected x-ray diffraction data from the liquid phase are shown in Fig. 1. The data were collected on beamline 9.1 at the Synchrotron

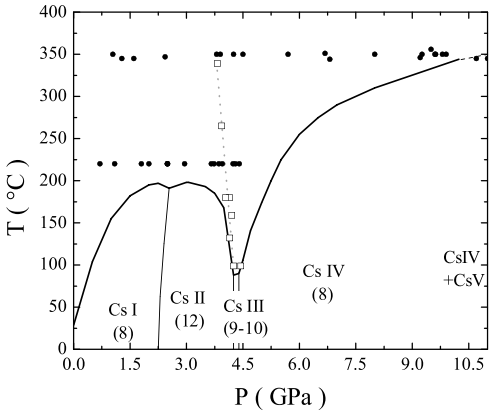

FIG. 1. The phase diagram of Cs up to 11 GPa [1,5]. The filled symbols show data collected on pressure increase and decrease at the fixed temperatures of $T = 220\,^{\circ}\mathrm{C}$ and $T = 350\,^{\circ}\mathrm{C}$. The open symbols show the thermodynamic path followed on heating a sample of Cs-III up to $T = 340\,^{\circ}\mathrm{C}$ at ~4.1 GPa. The dashed line through these points is a guide for the eye. The coordination numbers of the solid phases are given in parentheses below the name of the solid phase.

Radiation Source, Daresbury Laboratory, using a wavelength of 0.4654 Å [7]. The sample was contained in a diamond anvil cell equipped with W or Re gaskets [8], and the high temperatures were generated using a resistive heater. The pressure was determined using Mo as an internal calibrant [9]. The maximum diffraction angle of $2\theta \sim 36°$ corresponded to a maximum Q value of ~ 8.3 Å^{-1}.

The analysis procedure required to obtain the atom-atom structure factors from angle-dispersive x-ray diffraction data from liquids under extreme P-T conditions have been fully described by Eggert *et al.* and Kaplow *et al.* [10]. Spurious diffraction features, such as those from the Mo pressure calibrant, and the background scatter from the pressure cell were removed. The Bragg peaks from the Mo were easily identified and subtracted, and the background contribution was determined by measuring the diffraction pattern from the empty cell. The data were then normalized by the atomic form factor, taking into account the Compton scattering, the sample transmission coefficient, and a scale factor for the atomic form factor determined from the assumption that for sufficiently high Q, $S(Q) \sim 1$ [10]. Finally, for a homogeneous and isotropic medium such as a liquid or an amorphous solid, the structure factor can be written in terms of the atom-atom radial distribution function, $g(r)$, as

$$S(Q) - 1 = 4\pi\rho \int r^2[g(r) - 1]\frac{\sin Qr}{Qr}dr. \qquad (1)$$

This equation can be inverted to obtain $g(r)$, provided that the number density ρ is known [10,11].

Examples of the resulting $S(Q)$ data measured as a function of pressure at 220 °C and 350 °C near the melting curve are shown in Fig. 2. On increasing pressure at 220 °C, the profiles show a continuous change in shape. At low pressures the $S(Q)$ profiles are typical for a simple liquid which we have modeled as a system of hard spheres (HS) using the Percus-Yevick equation [11–13]. In such a liquid, it is known empirically that the height of the first peak in $S(Q)$ is between 2.5 and 3.0; that there are no shoulders on the high-Q side of this first peak; and that the ratio between the positions of the first and second peaks (Q_2/Q_1) is ~ 1.8 [14]. Our l-Cs profiles satisfy all three of these criteria up to 3.9 GPa and are in excellent agreement with the $S(Q)$ data of Tsuji *et al.* [6]. However, at pressures above 3.9 GPa, an asymmetry begins to appear on the high-Q side of the first peak; the intensity of the first peak decreases abruptly by ~ 0.2 at 3.9 GPa and approaches a value of ~ 1.8 at 9.8 GPa; and the ratio Q_2/Q_1 becomes almost pressure independent above 3.9 GPa, with a value of ~ 2.0. These changes all suggest that Cs is no longer a simple liquid above 3.9 GPa.

Further evidence of this change of character is observed in the density of the liquid. Below 3.9 GPa, this can be estimated using two different procedures. The position of the first peak of the $S(Q)$ of a liquid is very sensitive to pressure, as observed previously in l-Cs [6]. The shift with pressure of this peak can be related empirically to the change in the sample volume (and hence density) through the relationship $\frac{V_0}{V_P} = (\frac{Q_0}{Q_P})^{-3}$, where V_0,V_P, Q_0, and Q_P are the volumes and positions of the first peak at ambient pressure, and at a pressure P [6,12,13]. This empirical law has been used extensively at high pressure [6,13,14] and is applicable while the structure factor profile is that of a simple liquid. As a cross check, the specific volume was also obtained from the measured structure factors by fitting them using the HS model developed for liquid alkali metals [12]. In this model, the packing fraction η just above the melting curve is assumed to be constant and equal to 0.45 [12]. The specific volume and the hard sphere diameter (σ) were then obtained by a least-squares fit to the structure factors. η is related directly to the diameter of HS's and to the density via the relationship $\eta = \frac{\pi}{6}\rho\sigma^3$. The specific

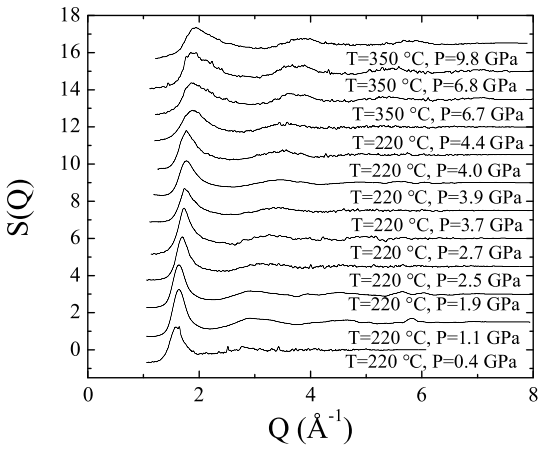

FIG. 2. Structure factors of l-Cs collected close to the melting curve in the range of pressure between 0.4 and 9.8 GPa. A constant offset of 1 has been used to separate the profiles.

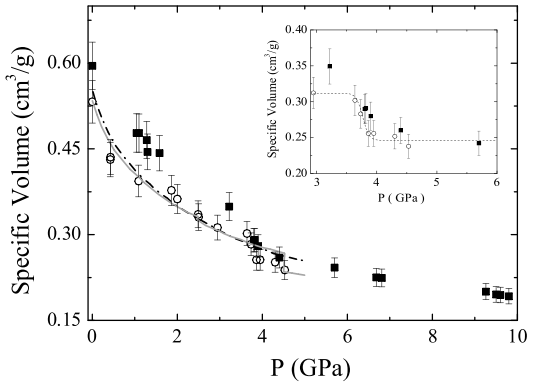

FIG. 3. The specific volume of l-Cs at $T = 220$ °C (open circles) and $T = 350$ °C (filled squares) as a function of pressure. The solid and dot-dashed lines are the specific volume data of the solid at 20 °C and liquid at 198 °C, respectively, from Ref. [1]. The inset shows an enlarged view of the data in the region 2.9 and 6 GPa. The dashed line is a guide for the eye.

volume of Cs below 3.9 GPa obtained using these two different methods agreed with each other to within 7%, and their average was used at each pressure.

However, neither of these methods can be used to determine the density above 3.9 GPa in the nonsimple regime. Up to 5.7 GPa the density of the liquid was estimated from the change in volume on melting reported in Ref. [1,5] and the density of the corresponding solid phases. From 5.7 to 9.8 GPa, the volume change on melting is not available in the literature. At the highest pressure of 9.8 GPa, the density of the solid was determined from the structure of crystalline Cs-IV at 9.8 GPa and 300 °C and the known slope of the melting curve at this pressure. It was also assumed that the change in entropy on melting at 9.8 GPa is the same as that at 5 GPa, the highest pressure at which it has been measured [1]. The resulting estimation of the specific volumes at 220 °C and 350 °C is shown in Fig. 3 and can be seen to be in very good agreement with those measured previously at 198 °C by Kennedy *et al.* [1]. At 220 °C, the specific volume of *l*-Cs decreases monotonically up to 3.7 GPa at which point it shows evidence of a sharp densification of 17(4)%. We note that this densification occurs at a lower pressure than the volume discontinuity of 12.5(2)% observed in the solid at the combined Cs-II → Cs-III → Cs-IV transitions [3] (which occur at 4.2 and 4.4 GPa at 20 °C). Unfortunately, we could measure the compressibility of the denser state up to only 4.4 GPa at 220 °C, only slightly higher than the pressure reached by Tsuji *et al.*. However, by raising the temperature to 350 °C (see Fig. 1), it was possible to extend the compressibility measurements of the liquid to ~10 GPa, as shown in Fig. 3. Below ~3 GPa, the specific volume of *l*-Cs at 350 °C is greater than that at 220 °C, as expected from thermal expansion. However, at higher pressures, the volumes at 220 °C and 350 °C are much more similar, suggesting that temperature has little effect on the specific volume at these pressures. To confirm this, we have measured the temperature evolution of $S(Q)$ at an (almost) constant pressure of 4.2 GPa, the pressure at which the melting temperature is lowest (Fig. 1).

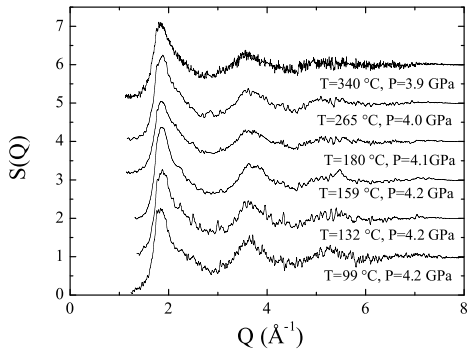

FIG. 4. Structure factors of *l*-Cs collected in the pressure range between 4.1 and 3.8 GPa and the temperature range between $T = 99$ °C and $T = 340$ °C.

The $S(Q)$ profiles obtained on heating from 99 °C up to 340 °C are shown in Fig. 4. The 99 °C profile exhibits a shoulder on the high-Q side of the first peak, and, although the shoulder becomes less pronounced at higher temperatures, the liquid remains nonsimple to the highest temperature. The position of the first peak of $S(Q)$ shows very little change with temperature, and the change in the specific volume heating from 99 °C to 340 °C at 4.2 GPa is only 0.003(1) cm^3/g. This thermal expansion is considerably smaller than that obtained on heating *l*-Cs from 220 °C to 340 °C below 2 GPa, where the specific volume changes by ~0.06(1) cm^3/g (see Fig. 3), and is consistent with the similar specific volumes observed at 220 °C up to 340 °C above 4 GPa.

As said previously, the $S(Q)$ data can be inverted to obtain the radial distribution function $g(r)$, and hence obtain both coordination numbers (C_{NN}) and the average nearest-neighbor distances (d), as illustrated in Fig. 5. The distance between nearest neighbors (d) was taken as the position of the first peak of $g(r)$, and C_{NN} was determined by integrating $g(r)$ up to the first minimum. The coordination number of *l*-Cs just above atmospheric pressure is ~12, in good agreement with the previous determination of Tsuji *et al.* [6], and slightly higher than the value of 11 expected for a system of hard spheres (as shown by the dotted horizontal line in Fig. 5). On initial compression at 220 °C, C_{NN} increases slightly with pressure while d compresses uniformly, both as expected for a simple liquid and

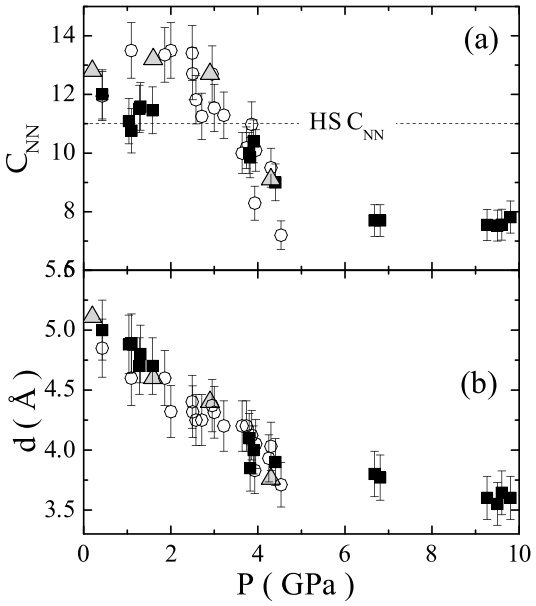

FIG. 5. (a) Coordination number C_{NN} of liquid Cs as a function of pressure. The horizontal dashed line is the coordination number (11) for a system of hard spheres. (b) The nearest-neighbor distance as a function of pressure. In both panels, the data collected at 220 °C and 350 °C are shown using open circles and filled squares, respectively, while the filled triangles are the data from the work of Tsuji *et al.* [6].

in agreement with Tsuji *et al.* [6] [Fig. 5(a)]. However, above ~2.5 GPa, C_{NN} begins to decrease, and becomes less than 11 at ~3.9 GPa, the pressure at which the $S(Q)$ profiles cease to be those of a simple liquid. C_{NN} decreases still further above 3.9 GPa, and, by 4.5 GPa, the coordination number is only 7 or 8 and this is maintained up to 9.8 GPa. The changes in coordination reported previously by Tsuji *et al.* [6] up to 4.3 GPa are in excellent agreement with the present results. The pressure dependence of the nearest-neighbor distance d is shown in Fig. 5(b). Up to 4.5 GPa it decreases almost uniformly with pressure, before becoming much less compressible once the low-coordination form is obtained above this pressure. The values of d from Tsuji *et al.* [6] up to 4.3 GPa are again in excellent agreement. The changes in the coordination and nearest-neighbor distance in the liquid can be compared to those that occur in the solid phases over the same pressure range. The two solid phases stable up to 3.6 GPa, Cs-I (bcc) and Cs-II (fcc), have coordination numbers of 8 and 12, respectively, compared to the coordination number of the simple liquid of 11–12 over this pressure range (0 to 3.6 GPa). The transitions from Cs-II to Cs-III and Cs-IV at 4.2 and 4.4 GPa, are accompanied by a 12.5(2)% increase in density, and a decrease in coordination number from 12 (Cs-II) to 9 or 10 (Cs-III) to 8 (Cs-IV) [3]. These changes in structure and coordination of the solid have long been attributed to an s-to-d electronic transition, and, at higher pressures, to dsp^3 hybridization of the electronic orbitals [2,4,15,16]. In particular, the relatively low eightfold coordination of Cs-IV has been attributed to the existence of directional bonding as a result of the occupation of d-orbitals. The structural changes in l-Cs over the pressure range 3.6–4.5 GPa are very similar, with a density increase of 17(4)% and a decrease in coordination number from ~11 to ~8. This close similarity in the behavior of the solid and liquid strongly suggests that the electronic phenomenon responsible for the changes in the solid is also occurring in the liquid. In particular, the reduced coordination number in the liquid suggests that there must be some form of preferential orientation within the liquid in order to reduce C_{NN} below the typical simple-liquid value of 11. Such a preferential orientation would arise from the existence of the hybridization of s, d, and p orbitals, and the resulting anisotropy in the local structure would then be in agreement with the asymmetry in the shape of the first peak of $S(Q)$ (see Fig. 3 and 4). The local structure would account for the asymmetry which occurs continuously over the pressure range 3.6–4.1 GPa where the liquid is denser than the solid.

The exact nature of this structural anisotropy, and hence an identification of the atomic orbitals involved, might be obtainable from *ab initio* simulations of the liquid phase, as has been done previously for liquid Rb [17,18]. We are currently conducting such simulations using a cluster of 264 atoms, the full results of which will be published separately.

In conclusion, liquid Cs undergoes a discontinuous change to a high-density low-coordination form at pressure above 3.9 GPa at 220 °C which cannot be modeled as a simple liquid. The similarities in the density and coordination change to those observed in the solid phases suggests that the cause of this densification is the same electron transfer and hybridization observed over the same pressure range in the solid phase.

We thank Professor R. J. Nelmes and Dr. J. S. Loveday for useful discussions and revisions. We thank also Dr. M. Roberts of Daresbury Laboratory for his assistance in setting up the 9.1 beam line at SRS. This work was supported by grants from EPSRC, funding from CCLRC, and beam time and other resources provided by SRS.

[1] G. C. Kennedy, A. Jayaraman, and R. C. Newton, Phys. Rev. **126**, 1363 (1962); A. Jayaraman, R. C. Newton, and J. M. McDonough, Phys. Rev. **159**, 527 (1967).
[2] K. Takemura, S. Minomura, O. Shimomura, Phys. Rev. Lett. **49**, 1772 (1982); K. Takemura and K. Syassen, Phys. Rev. B **32**, 2213 (1985).
[3] M. I. McMahon, R. J. Nelmes, and S. Rekhi, Phys. Rev. Lett. **87**, 255502 (2001).
[4] A. K. McMahan, Phys. Rev. B **29**, R5982 (1984).
[5] R. Boehler *et al.*, Physica B&C (Amsterdam) **140**, 233 (1986).
[6] K. Tsuji *et al.*, J. Non-Cryst. Solids **117-118**, 72 (1990); Y. Katayama and K. Tsuji, J. Phys. Condens. Matter **15**, 6085 (2003).
[7] R. J. Nelmes and M. I. McMahon, J. Synchrotron Radiat. **1**, 69 (1994).
[8] No reaction was observed between the Cs sample and the gasket materials. On returning the liquid samples to room temperature after heating, only diffraction peaks from crystalline Cs and the Mo pressure calibrant were observed.
[9] Y. Zhao *et al.*, Phys. Rev. B **62**, 8766 (2000).
[10] J. H. Eggert *et al.*, Phys. Rev. B **65**, 174105 (2002); R. Kaplow, S. L. Strong, and B. L. Averbach, Phys. Rev. **138**, A1336 (1965).
[11] J. P. Hansen and I. R. McDonald, in *Theory of Simple Liquids* (Academic Press, London, 1990).
[12] N. W. Ashcroft and J. Lekner, Phys. Rev. **145**, 83 (1966).
[13] G. Shen *et al.*, Phys. Rev. Lett., **92**, 185701 (2004).
[14] T. Hattori *et al.*, Phys. Rev. B **68**, 224106 (2003), and references therein; K. Tsuji *et al.*, J. Phys. Condens. Matter **16**, S989 (2004).
[15] M. M. Abd-Elmeguid, H. Pattyn, and S. Bukshpan, Phys. Rev. Lett., **72**, 502 (1994).
[16] I. Loa *et al.*, High Press. Res. **23**, 1 (2003).
[17] F. Shimojo *et al.*, Phys. Rev. B **55**, 5708 (1997).
[18] J. Chihara and G. Kahl, Phys. Rev. B **58**, 5314 (1998).